Fabrication of Aragonite Rosette Superstructure Through the Weak Interaction Between Nonionic Polymers and Ca^{2+}

Shuxian Shi,[1] Zhiqiang Su,[1] Hao Wei,[1] Xiaonong Chen[2]

[1]*Key Laboratory of Beijing City on Preparation and Processing of Novel Polymer Materials,
Beijing University of Chemical Technology, Beijing 100029, People's Republic of China*
[2]*Department of Biomaterials, College of Materials Science and Engineering, Beijing University of Chemical
Technology, Beijing 100029, People's Republic of China*

ABSTRACT: The controlled formation of aragonite by simple method under ambient condition is a big challenge for biomaterial scientists. In this article, we took poly (N-vinyl pyrrolidone) (PVP) as an example to investigate the influence of water-soluble nonionic polymers on the polymorphs of CaCO$_3$ via CO$_2$ diffusion method under ambient pressure and temperature, and found that the existence of PVP molecules favors the formation of aragonite with rosette superstructure. A possible mechanism is proposed that nonionic polymers can be doped into amorphous calcium carbonate (ACC) particles and further participate in the transformation process from ACC to aragonite and then promotes the formation of rosette superstructure through parallel aggregation by cross-linking the aragonite nuclei. The experiments of CaCO$_3$ crystallization in presence of poly(ethylene oxide) (PEO) and poly(vinyl alcohol) (PVA) confirmed the mechanism. © 2010 Wiley Periodicals, Inc. J Appl Polym Sci 117: 3308–3314, 2010

Key words: biomaterials; nucleation; poly(N-vinyl pyrrolidone); crystal morphology; calcium compounds

INTRODUCTION

Calcium carbonate (CaCO$_3$), as one of the most important biominerals, has attracted continuous attention in the past several decades, not only for its abundant content as biominerals, but also for various industrial applications as filler in paint, plastic, paper, and so forth.[1–3] Calcite, aragonite, and vaterite are the anhydrous crystalline phases of CaCO$_3$. In terms of thermodynamics, aragonite is a metastable polymorph of CaCO$_3$ and can be easily transformed into the most stable polymorph, calcite.[4] The strength and needle-shaped morphology of aragonite endue aragonite with the obvious reinforcement in composite materials.[5,6] However, aragonite with needle shape is not easily obtained in mild precipitation condition except in organism, or with an excess of inorganic ions, or controlled by polymer or surfactant with complicated structures.[7–9] Therefore, the controlled formation of aragonite with simple method under ambient condition is a big challenge for scientists.[10,11]

It is well known that organisms can easily control the process of biomineralization, which leads to well defined organic–inorganic hybrid materials with superior material properties, complex morphologies, and ordered structures.[12,13] Illumined by the biomineralization, many templates including langmuir monolayer,[14] self-assembled films,[15] bio- or synthetic macromolecules,[16] low molecular weight compounds,[17] and others, have been used to control the morphology and polymorphs of inorganic crystals.[18] Although it is widely accepted that the organic additives/matrixes play significant roles in mineralization process, the negative charge is necessary for the control of the organic additive/matrixes on the polymorph of calcium carbonate in the process of biomineralization.[19] Traditionally, the nonionic polymeric additives, such as PVP, were believed to have almost no effect on polymorphism selection.[20,21]

In this article, we examined the effect of the water-soluble nonionic polymers (PVP, PVA, and PEO) on the polymorph control of CaCO$_3$ by the so-called "vapor diffusion" method under mild condition. The results indicated that the weak interaction between nonionic polymers and Ca^{2+}/CaCO$_3$ nuclei can not only significantly influence the morphology of CaCO$_3$ but also lead to the fabrication of
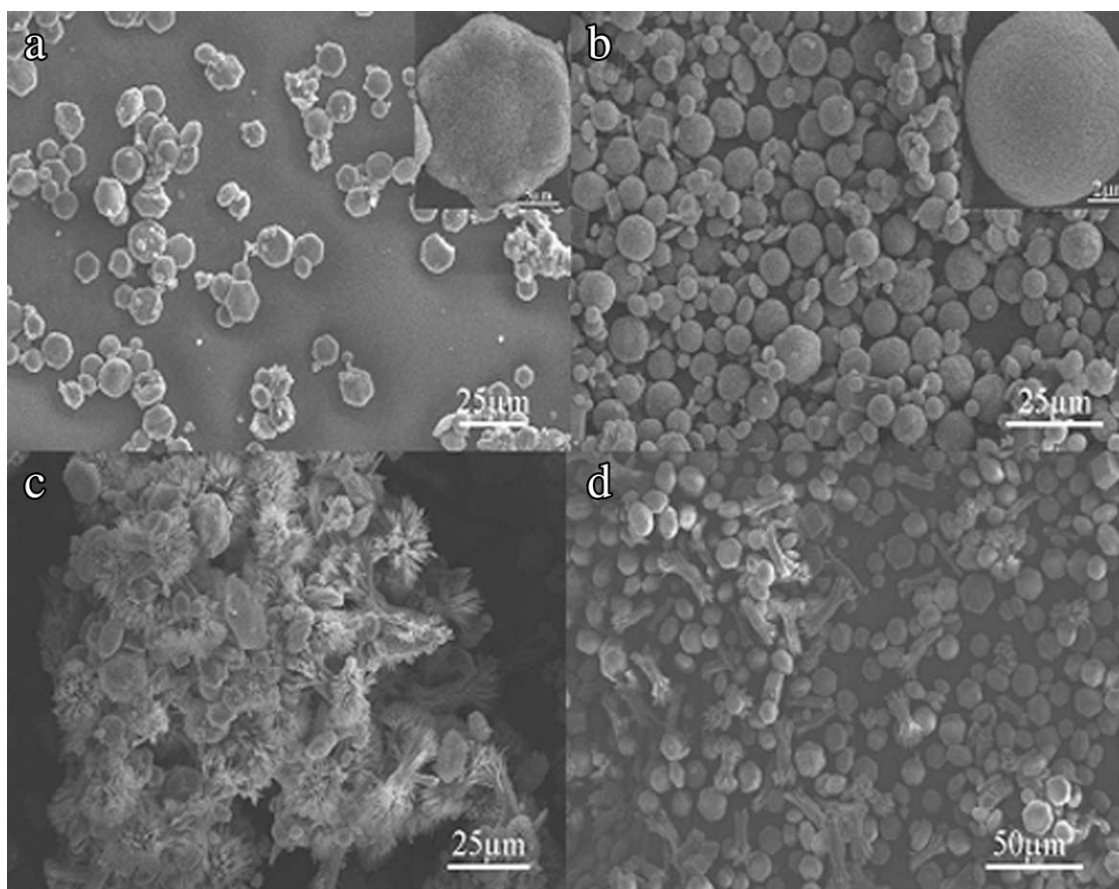
Figure 1 SEM images of $CaCO_3$ precipitate obtained by gas diffusion reaction after 18 h in 50 mL solution with different concentration of Ca^{2+} and PVP. (a) $[Ca^{2+}]$ = 50 mM, [PVP] = 100 ppm; (b) $[Ca^{2+}]$ = 50 mM, [PVP] = 500 ppm; (c) $[Ca^{2+}]$ = 50 mM, [PVP] = 1000 ppm; (d) $[Ca^{2+}]$ = 100 mM, [PVP] = 1000 ppm.

aragonite with rosette superstructure under slow and static condition. The possible effect of nonionic polymers on $CaCO_3$ precipitation was proposed: (1) the additives can be doped into synthenic ACC and participate the transformation process from ACC to aragonite[22,23]; (2) the additives crosslink the aragonite nuclei and promote the formation of rosette superstructure through parallel aggregation.[24]

EXPERIMENTAL SECTION

Calcium chloride, PEO (M_w = 10,000), PVP (M_w = 30,000), PVA (99–100% hydrolyzed, M_w = 86,000), and $(NH_4)_2CO_3$ with purity of 99.5% were purchased from Acros company (Geel, Belgium) and used without further purification.

The $CaCO_3$ crystallization experiments, as reported by Addadi et al.,[24] were carried out at room temperature (25 ± 1°C) in a desiccator (1000 mL). Two flasks (80 mL) were placed into the closed desiccator. One flask covered by punched Parafilm (ten holes) contained the mixture solution (50 mL) of calcium chloride ($CaCl_2$) and nonionic polymer. Some flash $(NH_4)_2CO_3$ about 2 g was placed into

other flask. The $CaCO_3$ particles were obtained by decomposition of $(NH_4)_2CO_3$ and subsequent vapor diffusion of CO_2 into $CaCl_2$/polymer solution. At the end of the experiments, $CaCO_3$ particles were collected, washed, and dried in vacuum at 40°C.

$CaCO_3$ samples were Au-coated prior to examination by a Hitachi S-4300 scanning electron microscope (SEM), fitted with a field emission source and operated at an accelerating voltage of 15 kV. X-ray diffraction (XRD) measurements were conducted using a Rigaku D/max-2400 powder X-ray diffractometer with Cu Kα radiation (40 kV, 120 mA), and 0.02° step and 2 theta range of 20–60° were selected to analyze the crystal structure. FT-IR spectroscopic measurements were performed on a IFS-66v/S FTIR spectrometer (Bruker), with scanning times of 32, and resolution of 4 cm^{-1}.
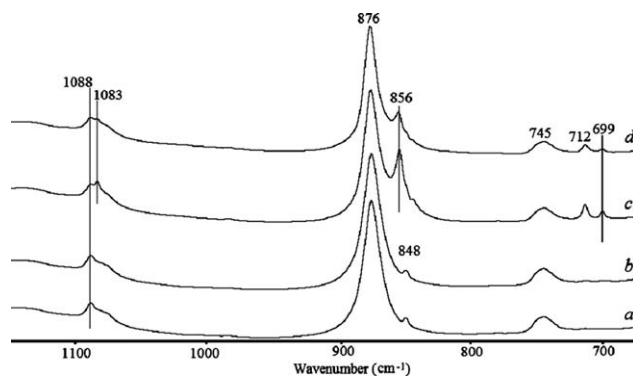
RESULTS AND DISCUSSION

In this article, we first take PVP as an example to investigate the influence of water-soluble nonionic polymers on the crystallization behavior of $CaCO_3$ via CO_2 diffusion method by decomposition of $(NH_4)_2CO_3$. Figure 1 displays the SEM images of
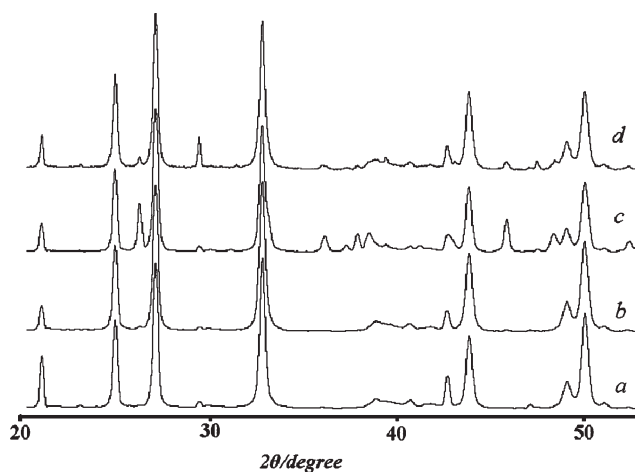
Figure 2 XRD results of CaCO₃ precipitate obtained by gas diffusion reaction after 18 h in 50 mL solution with different concentration of Ca^{2+} and PVP. (a) $[Ca^{2+}]$ = 50 mM, [PVP] = 100 ppm; (b) $[Ca^{2+}]$ = 50 mM, [PVP] = 500 ppm; (c) $[Ca^{2+}]$ = 50 mM, [PVP] = 1000 ppm; (d) $[Ca^{2+}]$ = 100 mM, [PVP] = 1000 ppm.

Figure 3 IR results of CaCO₃ precipitate obtained by gas diffusion reaction after 18 h in 50 mL solution with different concentration of Ca^{2+} and PVP. (a) $[Ca^{2+}]$ = 50 mM, [PVP] = 100 ppm; (b) $[Ca^{2+}]$ = 50 mM, [PVP] = 500 ppm; (c) $[Ca^{2+}]$ = 50 mM, [PVP] = 1000 ppm; (d) $[Ca^{2+}]$ = 100 mM, [PVP] = 1000 ppm.

CaCO₃ particles obtained from PVP/CaCl₂ mixed solution. It is obvious that the variation of CaCO₃ crystal morphology depends on the concentrations of both PVP and CaCl₂. In the presence of 100 ppm PVP and 50 mM CaCl₂, most of the CaCO₃ particles showed well hexagonal symmetry, similarly to the morphology of CaCO₃ obtained in the absence of PVP. Cölfen proved that this morphology was formed by the aggregation of nanoparticles via an oriented attachment mechanism.[25] This oriented attachment toward larger crystalline is currently identified to 'mesocrystal' formation.[26] However, at higher PVP concentration of 500 ppm, the classical spherical particles appear as shown in Figure 1(b).[27,28] XRD and IR results (Fig. 2), indicate that both hexagonal and spherical crystals are vaterite.

Interestingly, further increasing PVP concentration to 1000 ppm leads to a great deal of particles with rosette superstructure which is formed by the radial growth of needle crystal from the central section, and the central part is very compact in one dimension. The structure of the resulting CaCO₃ was analyzed by XRD (Fig. 2). The corresponding pattern of the sample displays the diffraction peaks of both vaterite and aragonite [Fig. 2(c)]. The diffraction peaks (2θ) of aragonite at 26.17°, 27.40°, 32.74°, 36.10°, 37.24°, 37.86°, and 38.46°, correspond to the (*hkl*) indices of (111), (021), (121), (200), (031), (112), and (113), respectively. As for the hexagonal particles observed with SEM, the diffraction peaks of vaterite appear at 20.92° (004), 24.84° (110), 27.04° (112), and 32.72° (114) [Fig. 2(a,b)]. The identification of the phase of these particles was also confirmed by FTIR spectroscopy (Fig. 3), showing characteristic vibrational bands at 699, 712, 856, and 1083 cm⁻¹ for

aragonite, 745 and 848 cm⁻¹ for vaterite. To explore the influence of concentration of Ca^{2+} on the selectivity of the crystal morphology, the experiment of CaCO₃ crystallization via increasing $[Ca^{2+}]$ to 100 mM with fixing PVP concentration at 1000 ppm was carried out. The SEM observations [Fig. 1(d)], IR spectra (Fig. 3), and XRD analysis (Fig. 2) all suggest that the particles with rosette superstructure are mixtures of vaterite and aragonite. This fact indicates that PVP will favor the formation of aragonite, which is generally formed at high temperature or at room temperature with the addition of Mg^{2+}.[7,8]

However, in a long run, the water-soluble non-ionic polymers are believed to have seldom influence on the polymorph control of CaCO₃. Our previous work[20] also confirmed that PVP has no effect on the polymorph control of CaCO₃ under stirring condition. So we wonder what results in the formation of aragonite via CO₂ diffusion method? Based on a generally accepted fact that the polymorph control of inorganic minerals in presence of organic additives is attributed to the interaction between organic
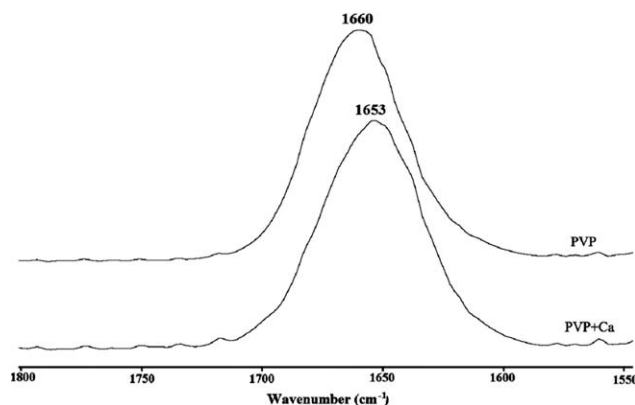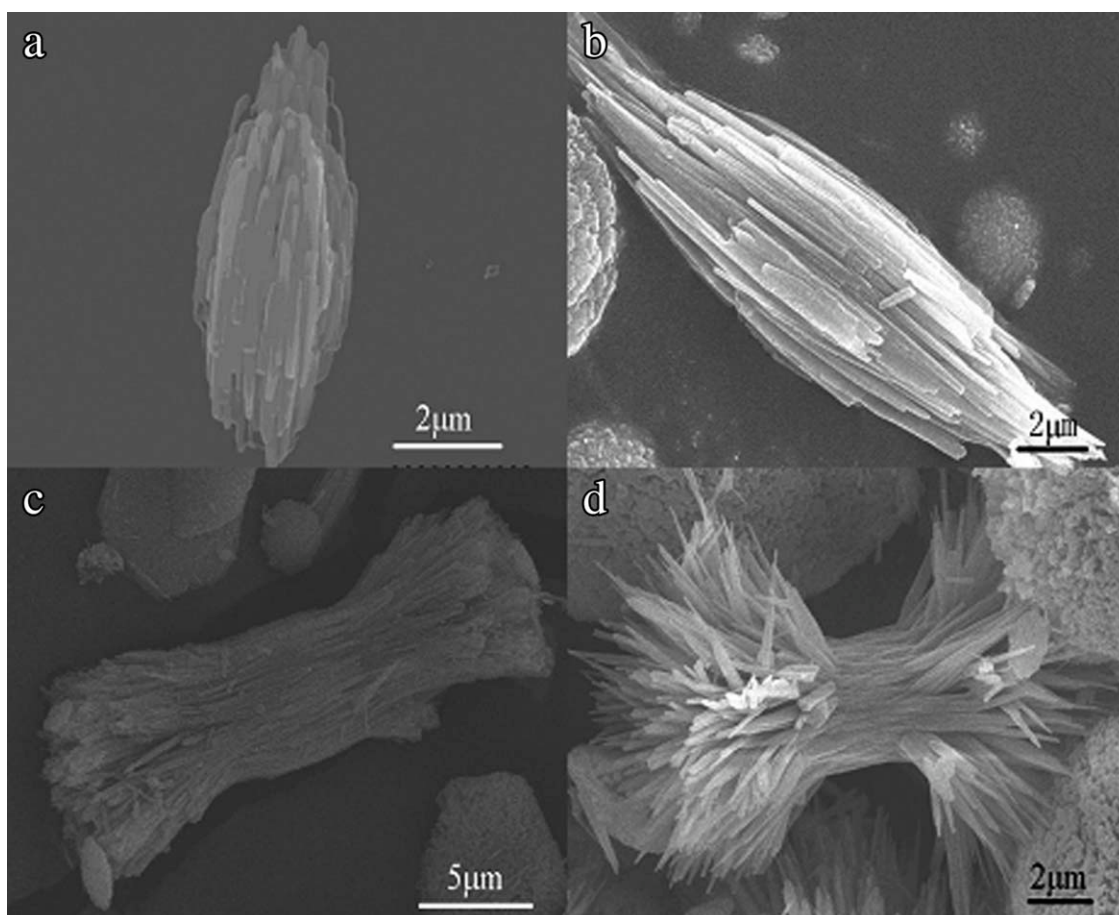

Figure 4 FT-IR spectra of pure PVP and mixture of PVP and CaCl₂ in the range of 1800–1550 cm⁻¹.
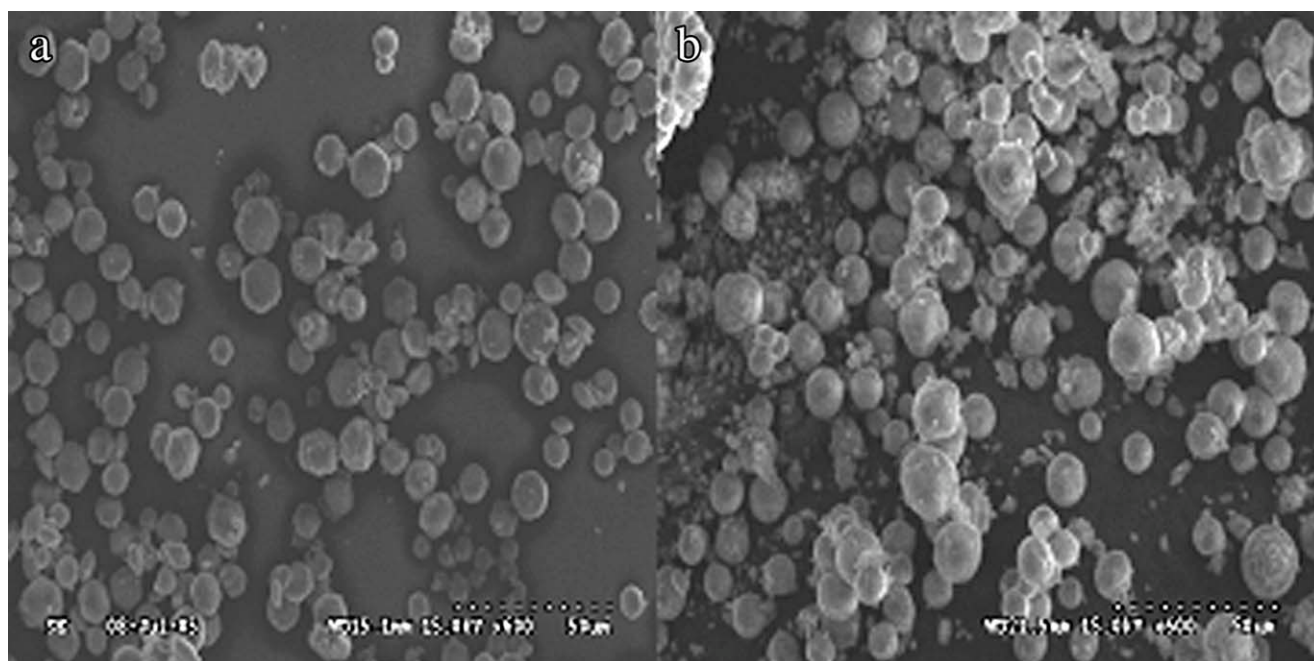
Figure 5 SEM images of $CaCO_3$ precipitate obtained by gas diffusion reaction after 18 h in 50 mL solution. (a) $[Ca^{2+}]$ = 50 mM, [PVP] = 1000 ppm; (b) $[Ca^{2+}]$ = 50 mM, [PVP] = 1000 ppm, $[KI_3]$ = 40 mM.


Figure 6 SEM images clearly demonstrated that the $CaCO_3$ particles with rosette superstructure are developed starting from small needle-like particle (a) and growing to form shuttles (b), rods(c), and finally assembling into rosette particles (d) by parallel aggregation.

additives and the inorganic ion/crystal nuclei,[16-18] we presume that there may be the interaction between PVP and Ca^{2+}, which leads to the formation of aragonite. FT-IR spectroscopy was used to confirm such interaction. In PVP-$CaCl_2$ system, a clear IR band shift of the carbonyl stretching vibration of PVP from 1660 to 1653 cm^{-1} (Fig. 4) indicates interactions between PVP molecules and Ca^{2+} ions.[29] Moreover, since I_3^- can strongly interact with the carbonyl groups in PVP molecules,[30] we have the reason to believe that the addition of I_3^- ions into PVP–$CaCl_2$ solution will shield or decrease the interaction between the carbonyl group of PVP and Ca^{2+} ion, which may result in the disappearance of aragonite superstructure. As predicted, when 2 mL of 40 mM KI_3 solution was added, the aragonite superstructure vanished and only spherical particles appeared (Fig. 5). Thus, a conclusion can be drawn that weak interaction between PVP and Ca^{2+}/$CaCO_3$ nuclei play an important role in the formation of aragonite.

In an attempt to understand the formation mechanism of aragonite with rosette-like superstructure, high-magnified SEM images of $CaCO_3$ precipitation in different growing stages were obtained and shown in Figure 6, which reflect the formation procedure of rosette superstructure in presence of non-ionic polymer PVP. At the initial stage, the small olive-like particles [Fig. 6(a)] were first formed. It is found that the particles are composed of needle-like particles via parallel aggregation.[31] With extension of time, the small olive-like particles gradually grow bigger [Fig. 6(b)] and the two ends turn up to form thread bundles [Fig. 6(c)]. Finally, although the needle-like particles still parallelly aggregate along the long axis in the influence of PVP, an obvious angle is formed between the end and middle in the crystal bundles, resulting in the radial growth at the end of rosette-like particles [Fig. 6(d)].

According to the above experimental observations, we propose a possible mechanism for the formation of aragonite particles with rosette superstructure (Fig. 7), which displays the role of PVP on nucleation, growth, and ordered parallel aggregation to a rosette superstructure. FT-IR result has proved that in $CaCl_2$/PVP solution, Ca^{2+} ions spontaneously interact with carbonyl functional groups on PVP molecular chains. It is rational that the interaction will lead to the formation of Ca^{2+}–PVP complex and the "locally supersaturated" in solution, i.e., relatively higher concentration of Ca^{2+} in localized region in the bulk solution. As a result, the K_{sp} of $CaCO_3$ is primarily attained in the localized supersaturated region in solution, and then nucleation of $CaCO_3$ particles occurs [Fig. 7(a)] as CO_2 gas diffuses into solution. Although it is generally believed that the nonionic polymer as PVP have little influence on the morphology and crystalline of calcium carbonate
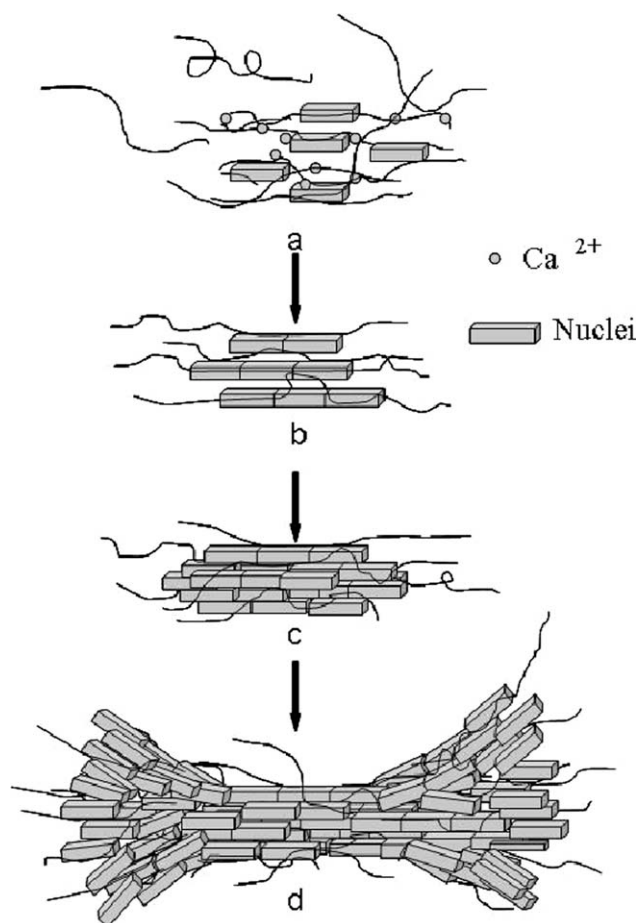
Figure 7 Possible mechanism for the formation of aragonite with rosette superstructure by the parallel aggregation of aragonite crystallites. (a) Nucleation of aragonite in the complex of PVP and Ca^{2+}, (b) growth of aragonite in the complex of PVP and Ca^{2+}, (c) parallel aggregation of needle aragonite depending on interaction between PVP, and (d) radical growth of crystal bundles.

under both dynamic and static conditions,[32,21] our present results indicate that PVP can induce the formation of aragonite nuclei via vapor diffusion method. With continuous diffusion of CO_2 into solution, the $CaCO_3$ nuclei will connect each other and grow to needle-like particles [Fig. 7(b)]. Because of the high surface energy and the connection via PVP, the fresh nuclei of $CaCO_3$ particles will spontaneously aggregate parallel to long axis direction of needle and form shuttle-shaped particles [Fig. 7(c)]. Moreover, polymer chains should adsorb on crystal surface to minimize the surface energy. So at the end part of the shuttle-like particle, PVP chains may adsorb on it and the crystal exhibits the radial growth manners. At the same time, new $CaCO_3$ nuclei will form along PVP molecules with the more CO_2 gas diffusing into $CaCl_2$ solution, resulting in the formation of rosette aragonite particles. Ultrasonic treatment to the final aragonite aggregates destroyed the rosette structure and subsequently
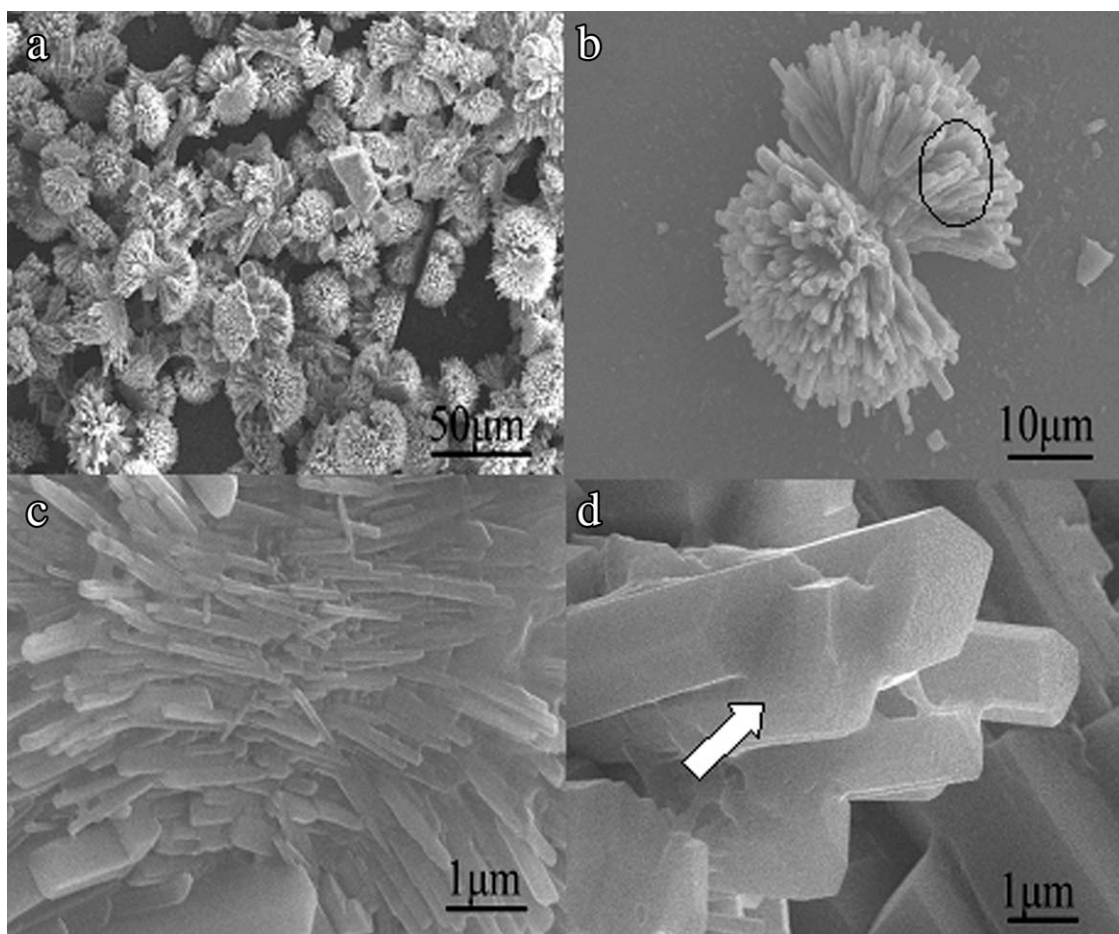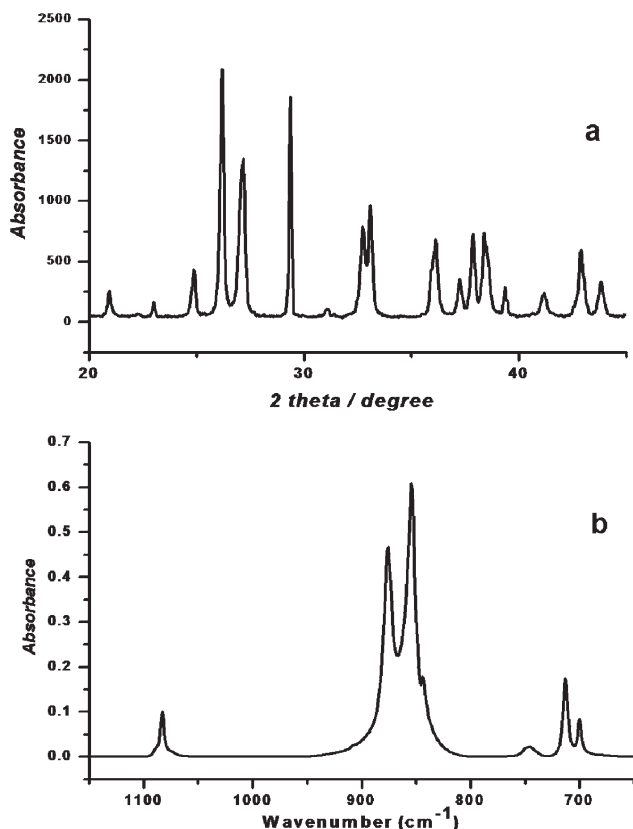
Figure 8 SEM images of CaCO$_3$ precipitate obtained by gas diffusion reaction after 18 h in 50 mL solution. The concentrations of Ca^{2+} and PVP are 50 mM and 1000 ppm, respectively. (c) The magnified image of the central part of the rosette supercrystal. (d) The magnified image of the part signed in (b).

separated needle-like crystals were obtained, suggesting the parallel stacking of aragonite crystallites to superstructures through weak interaction between PVP molecules and CaCO$_3$ nuclei [Fig. 7(d)]. Based on these discussions, we believe that if there is weak interaction between water-soluble nonionic polymers and Ca^{2+}/ CaCO$_3$ nuclei, the rosette-like supercrystal will form by the CO$_2$ diffusion method.

To further confirm this point, PVA and PEO were chosen as two kinds of nonionic polymers with different interaction with Ca^{2+} or CaCO$_3$ nuclei to control the crystallization of CaCO$_3$. Because PEO has neither specific interaction nor nonspecific adsorption ability with Ca^{2+},[33] we can presume that PEO should have no influence on the polymorph control of CaCO$_3$. The corresponding SEM results indicated that vaterite particles with well hexagonal symmetry were produced only in this case, just the same as in the absence of any organic additive. Therefore, the interaction between the polymers and Ca^{2+} or CaCO$_3$ nuclei is the precondition to control the morphology and polymorph of inorganic crystals.

Compared with PEO, one pertinent characteristics of PVA in water is its tendency to adsorb nonspecifically onto solid surface.[34] As revealed by Kato's report,[35] PVA matrix can favor the formation of aragonite film because the distance between the hydroxyl group of crystalline PVA is almost equal to that between calcium ions in the *ab* plane of aragonite.[36] Therefore, the introduction of PVA into the system of CaCO$_3$ crystallization will probably lead to the formation of rosette-shape aragonite crystal similar to PVP system. The corresponding SEM images (Fig. 8), XRD, and IR (Fig. 9) results support this point of view. Figure 8(a,b) revealed that the particles obtained in the presence of PVA display the rosette morphology, which is similar to the particles in the presence of PVP. The magnified image of central part of the rosette supercrystal, shown in Figure 8(c), also suggests that this structure is formed by parallel aggregate of small needle-like particles along the long axis. Furthermore, PVA can be obviously found on the surface of needle-like particles from the magnified image [Fig. 8(d)] of the part marked in Figure 8(b). The corresponding XRD

Figure 9 XRD (a) and IR (b) results of CaCO$_3$ precipitate obtained by gas diffusion reaction after 18 h in 50 mL solution. The concentrations of Ca^{2+} and PVA are 50 mM and 1000 ppm, respectively.

and IR analyses confirmed the formation of aragonite (Fig. 9).

CONCLUSIONS

We have demonstrated that it is possible to generate aragonite crystals in the presence of nonionic polymers by gas-diffusion technique under ambient pressure and temperature. In the mineralization process, nonionic polymer can be doped into ACC particles and control the nucleation and morphology of CaCO$_3$ via weak interaction between nonionic polymer and Ca^{2+}/CaCO$_3$ nuclei, yielding rosette superstructure by parallel aggregation of CaCO$_3$ crystallites.

References

1. Mann, S.; Ozin, G. A. Nature 1996, 382, 313.
2. Yang, H.; Coombs, N.; Ozin, G. A. Nature 1997, 386, 692.
3. Ahmadi, T. S.; Wang, Z. L.; Green, T. C.; Henglein, A.; El-Sayed, M. A. Science 1996, 272, 1924.
4. Watabe, N. In Progress in Crystal Growth Characteristics; Pamplin, B. R., Ed.; Pergamon Press: London, England, 1981; Vol. 4.
5. Cardarelli, F. Materials Handbook: A Concise Desktop Reference; Springer-Verlag: London, 2000.
6. Zaremba, C. M.; Morse, D. E.; Mann, S.; Hansma, P. K.; Stucky, G. D. Chem Mater 1998, 10, 3813.
7. Kitano, Y. Bull Chem Soc Jpn 1962, 35, 1973.
8. Wilbur, K. M.; Bernhardt, A. M. Biol Bull 1984, 166, 251.
9. Chen, S. F.; Yu, S. H.; Jiang, J.; Li, F.; Liu, Y. Chem Mater 2006, 18, 115.
10. Falini, G.; Albeck, S.; Weiner, S.; Addadi, L. Science 1996, 271, 67.
11. Belcher, A. M.; Wu, X. H.; Christensen, R. J.; Hansma, P. K.; Stucky, G. D.; Morse, D. E. Nature 1996, 7, 689.
12. Bommel, K. J. C. V.; Friggeri, A.; Shinkai, S. Angew Chem Int Ed 2003, 42, 980.
13. Cölfen, H.; Mann, S. Angew Chem Int Ed 2003, 42, 2350.
14. Mann, S.; Heywood, B. R.; Rajam, S.; Birchall, J. D. Nature 1988, 334, 692.
15. Küther, J.; Tremel, W. Chem Commun 1997, 37, 1593.
16. Levi, Y.; Albeck, S.; Brack, A.; Weiner, S.; Addadi, L. Chem Eur J 1998, 4, 389.
17. Didymus, J. M.; Oliver, P.; Mann, S.; Devires, A. L.; Hauschka, P. V.; Westbroek, P. J Chem Soc Faraday Trans 1993, 89, 2891.
18. Naka, K.; Chujo, Y. Chem Mater 2001, 13, 3245.
19. Calvert, P.; Mann, S. Nature 1997, 386, 12.
20. Wei, H.; Shen, Q.; Zhou, Y.; Wang, D.; Xu, D. J Cryst Growth 2003, 250, 516.
21. Kim, W.; Robertson, R. E.; Zand, R. Cryst Growth Des 2005, 5, 513.
22. Gower, L. B.; Odom, D. J. J Cryst Growth 2000, 210, 719.
23. Zhou, G. T.; Yao, Q. Z.; Ni, J.; Jin, G. Am Mineral 2009, 94, 293.
24. Addadi, L.; Mradian, J.; Shay, E.; Marounas, N. G.; Weinner, S. Proc Natl Acad Sci USA 1987, 84, 2732.
25. Gehrke, N.; Cölfen, H.; Pinna, N.; Antonietti, M.; Nassif, N. Cryst Growth Des 2005, 5, 1317.
26. Cölfen, H.; Antonietti, M. Angew Chem Int Ed 2005, 44, 2.
27. Privaman, T.; Goia, D. V.; Park, J.; Matigevic, E. J Colloid Interface Sci 1999, 213, 36.
28. Ogino, T.; Suzuki, T.; Sjwada, K. Geochim Cosmochim Acta 1987, 51, 2757.
29. Rivas, L.; Pereira, E. D.; Moreno-Villoslanda, I. Prog Polym Sci 2003, 28, 173.
30. Liu, C.; Cui, S.; Wang, Z.; Zhang, X. J Phys Chem B 2005, 109, 14807.
31. Tai, C. Y.; Chen, F. B. AIChE J 1998, 44, 1790.
32. Wei, H.; Shen, Q.; Zhao, Y.; Wang, D.; Xu, D. J Cryst Growth 2004, 260, 511.
33. Fleer, G. J.; Scheutjens, J. M. H. M.; Cohen Stuart, M. A. Colloids Surf 1988, 31, 1.
34. Barton, A. F. M. CRC Handbook of Polymer-Liquid Interaction Parameters and Solubility Parameters; CRC Press: Boca Raton, FL, 1990.
35. Hosoda, N.; Sugawara, A.; Kato, T. Macromolecules 2003, 36, 6449.
36. Bunn, C. W. Nature 1948, 161, 929.